The Impact of HIPPARCOS on Our Knowledge of Nearby Stars

Hartmut Jahreiß, Roland Wielen, Burkhard Fuchs
Astronomisches Rechen-Institut,
Mönchhofstraße 12-14, D-69120 Heidelberg, Germany

1 Introduction

In recent years an enormous revival of the research on nearby stars can be recognized. There is for one part, the search for brown dwarfs and extrasolar planetary companions. For the other part, there are the very important results of the Hipparcos satellite (ESA, 1997; Jahreiß and Wielen, 1997). The consequences of the latter results are discussed in this paper.

At present our data-base on nearby stars comprises altogether more than 5 800 entries. e.g. accepted, suspected, and rejected nearby (search limit about 25 pc) objects. From these almost 3 400 stars were observed by Hipparcos, i.e. 90 per cent of the possible targets, taking into account the magnitude limit (V $\approx$ 12$^{\rm m}$) of the satellite. For less than 40 stars Hipparcos observed the wrong target star or gives no astrometric result.

The mission of the Hipparcos satellite was not really designed to find new hitherto unknown nearby stars. Aside from the Hipparcos 'survey' ($V_{\rm lim} \approx 7\overset{\rm m}{.}5$) only known or suspected nearby stars entered the Hipparcos Input Catalogue with high priority. Nevertheless, Hipparcos *found* 145 new stars within 25 pc and in addition 37 previously unkown companions. Among the new stars LP 816-60 (= Hip 103 039) is the nearest one at 5.5 pc; all other are beyond 10 pc.

2 Hipparcos versus ground-based parallaxes

The fourth edition of the General Catalogue of Trigonometric Stellar Parallaxes (van Altena et al., 1995) represents the outcome of one century of ground-based trigonometric parallax work. It contains 1 973 *nearby* systems (altogether 2 445 stars), i.e. stars with ground-based trigonometric parallaxes $\pi_g \geq 40$ mas. 1 452 of these systems, i.e almost all stars brighter than 12$^{\rm m}$, the approximate magnitude limit of the Hipparcos satellite, were measured by Hipparcos. The median standard error of the corresponding Hipparcos parallax π_H is 1.15 mas compared to an error of 8.8 mas for the π_g. In Figure 1 the differences $\pi_H - \pi_g$ are plotted against π_H. The error bars represent Hipparcos errors. Among the very nearby stars, not shown here, noticable differences occur only for a few southern stars without modern ground-based parallaxes. It is evident that there are only a very few stars with large Hipparcos errors. Since we are dealing with a volume limited sample stars with positive parallax errors in π_g are preferentially included. The larger the errors in π_g the more stars are erroneously within the distance limit. Hipparcos has proven that only 66 per cent of the stars with $\pi_g \geq 40$ mas are really within 25 pc.

During the compilation of the Catalogues of Nearby Stars (CNS1, CNS2) Wilhelm Gliese (1957, 1968) tried to reduce this well known bias by incorporating spectroscopic and photometric distance estimates to improve poor trigonometric parallaxes. Since then the progress obtained

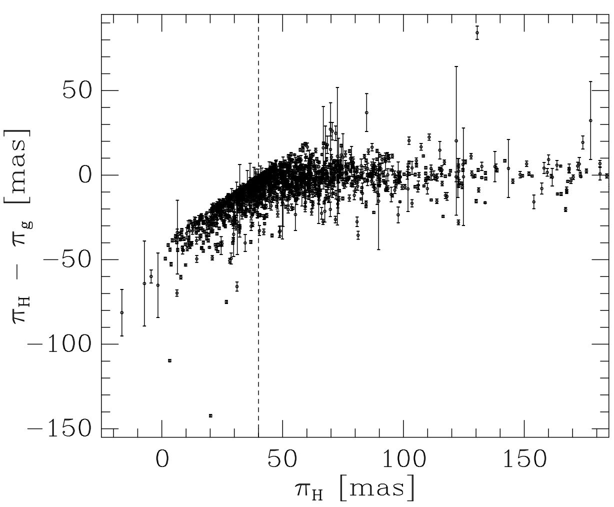

Figure 1: Trigonometric parallax differences $\pi_H - \pi_g$ versus the Hipparcos parallaxes for the 1 452 stars with $\pi_g \geq 40$ mas. The dashed line marks the distance limit of the CNS.

in photometric and spectroscopic work offers a variety of additional distance estimates. This yields a further reduction of the bias in the most recent ground-based version of CNS3. In Table 1 the number of CNS3 stars in different distance intervals can be compared with the corresponding CNS4 values. The CNS4 is based on Hipparcos data. Of course, these figures

Table 1: CNS3 versus CNS4 (number of stars and number density in different distance intervals)

r [pc]	0 – 5	5 – 10	10 – 20	20 – 25	0 – 25
CNS3	65	268	1 593	949	2 875
CNS4	61	257	1 552	1 126	2 996
$*/[pc^3]$	0.116	0.070	0.053	0.035	0.046

give only a superficial impression of the real impact of Hipparcos, and may even be misleading: the drop from 65 to 61 stars within 5 pc, for example, is mainly due to a tiny outward shift of the triple system ϵ Eri to 5.04 pc. The larger number of CNS4 stars in the 20 to 25 pc shell can be explained by the fact that Hipparcos found not only 85 new stars in this distance interval, but increased also many distances of nearer stars (see Figure 1). In general, apart from some giants erroneously classified as dwarfs, the ground-based parallaxes were not seriously wrong.

In a similar way also the Mc Cormick K and M dwarfs found in a spectroscopic survey (Vyssotsky, 1963) were indeed more or less *nearby* according to Hipparcos: For 16 of these dwarf stars the measured Hipparcos parallax was smaller than 10 mas, and a subsequent check proofed that in all of these cases Hipparcos observed a wrong target.

3 The colour-magnitude diagram

The extraordinary improvements achieved by Hipparcos are most impressively demonstrated in the colour-magnitude diagram of Figure 2. B–V was chosen as colour index producing an

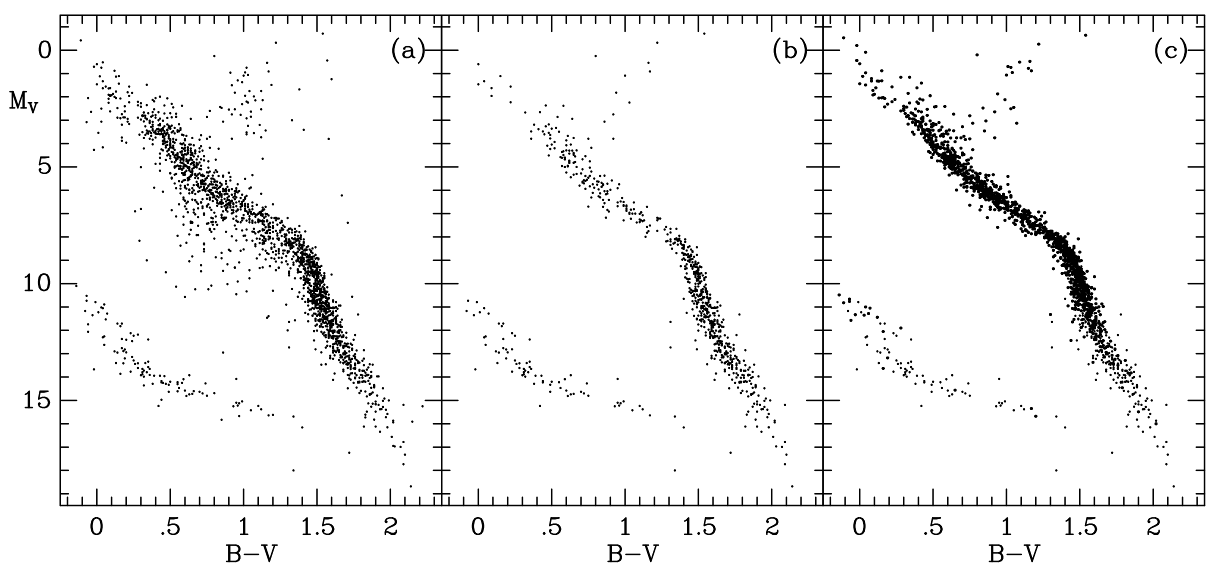

Figure 2: CM diagrams for nearby stars ($r \leq 25\,pc$): (a) CNS3: all stars with ground-based trigonometric parallaxes (b) CNS3 stars with $\sigma_\pi/\pi < 0.10$. (c) CNS4: all nearby stars with good ($\sigma_\pi/\pi < 0.10$) parallaxes (1 411 π_H and 350 π_g).

almost complete picture of the solar neighbourhood. For the CNS4 stars only about 200 good B–V measurements could be obtained from the Tycho experiment, the remaining colours are from ground-based measurements, and for the fainter stars some incorrect identifications are possible.

To summarize, the upper part of the CM diagram is now almost exclusively dominated by the Hipparcos parallaxes. Due to the fact that the CNS4 is practically complete for $M_V \leq 8^{\rm m}$ it presents also the true distribution of the stars in the solar neighbourhood. On the other hand the lower part must still rely on ground-based parallaxes and becomes rather rapidly incomplete for fainter magnitudes.

4 The stellar luminosity function

The completeness of the absolutly bright stars in the CNS4 within 25 pc allows a determination of the luminosity function in the bright part from twice the volume available in Wielen et al. (1983). For $M_V \geq 8^{\rm m}$ a restriction to declinations north of –30° yields a significantly higher star density. A reduction of the distance limit to 20 pc is appropriate for $M_V \geq 9^{\rm m}$. This was already the case in Wielen et al. (1983), and also for the fainter magnitude bins the former completeness limits were applied. There were no strong reasons for a change of these limits. Only for $M_V \geq 18^{\rm m}$ slightly different limits were chosen. The recently detected brown dwarf companion of Gl 229 was not yet included. According to a HST measurement Gl 229B has $M_V = 26^{\rm m}$.

The resulting luminosity function $\Phi(M_V)$ is presented in Table 2. Column 2 and 3 show the chosen completeness limits in distance and declination, and column 4 gives the number of CNS4 stars within these limits. Poisson errors give the statistical uncertainty ε_Φ (column 6).

Table 2: The stellar luminosity function for all stars $\Phi(M_V)$ and for stars on or near the main sequence $\Phi_{ms}(M_V)$ (Unit: number of stars within 20 pc in 1 mag bin)

M_V	r [pc]	δ	N	$\Phi(M_V)$	ε_Φ	$\Phi^{83}(M_V)$	$\Phi_{ms}(M_V)$
–1	25	all	2	1	1	1	0.5
0	25	all	8	4	2	4	3
1	25	all	22	11	3	14	8
2	25	all	31	16	3	24	14
3	25	all	80	41	5	43	37
4	25	all	112	57	6	78	53
5	25	all	191	98	7	108	98
6	25	all	195	100	7	121	100
7	25	all	192	98	7	102	98
8	25	$\geq -30°$	164	112	9	132	112
9	20	$\geq -30°$	105	140	14	159	140
10	10	$\geq -30°$	22	235	50	245	235
11	10	$\geq -30°$	28	300	57	341	277
12	5	$\geq -30°$	5	427	191	512	427
13	5	$\geq -30°$	4	341	171	597	256
14	5	$\geq -30°$	4	341	171	427	256
15	5	$\geq -30°$	5	427	191	427	427
16	5	$\geq -30°$	4	341	171	299	341
17	5	$\geq -30°$	2	171	121	299	171
18	10	$\geq -30°$	7	75	28	>16	75
19	10	$\geq -30°$	4	43	21	>16	43
20						> 5	
21	25	all	3	>0.4	0.2	> 5	>0.4
22							
23							

The corresponding luminosity function $\Phi_{ms}(M_V)$ for stars on or near the main sequence (white dwarfs and red giants were excluded) is given in column 8.

It is immediately evident that the bright end, $M_V \leq 7^m$, of $\Phi(M_V)$ is systematically lower than $\Phi^{83}(M_V)$ the luminosity function from Wielen et al. (1983) in column 7. Indeed, the present luminosity function yields about 15 per cent fewer bright stars. Only marginally affected by Hipparcos, there are also fewer stars around the maximum of the luminosity function. Yet, in these faint magnitude intervals the scatter of the determination is rather high due to the small volume sampled.

The Hipparcos catalogue is complete over the whole sky at least for $V \leq 7\overset{m}{.}3$. This allows a determination of the stellar luminosity function in a much larger sample volume ($r_{max} = 50$ pc) for the brightest absolute magnitudes. The result $\Phi_{50}(M_V)$ (see Table 3) is in excellent agreement with the LMF determined from the CNS4, except for the faintest magnitude bin. A different binning shows that the density deviates only in the last half-magnitude bin $M_V = (3\overset{m}{.}0, 3\overset{m}{.}5)$.

Table 3: The stellar luminosity function $\Phi_{50}(M_V)$ (sampling distance 50 pc)

M_V	N_{50}	$\Phi_{50}(M_V)$	$\varepsilon_{\Phi_{50}}$	N_{25}	$\Phi_{25}(M_V)$	$\varepsilon_{\Phi_{25}}$
–1	17	1.1	0.3	2	1	1
0	53	3.4	0.5	8	4	2
1	174	11.1	0.8	22	11	3
2	259	16.6	1.0	31	16	3
3	553	35.4	1.5	80	41	5

Combining the luminosity function $\Phi_{ms}(M_V)$ with a modern mass-luminosity relation and adding appropriate mass estimates for white dwarfs and old giants yields $0.039\,\mathcal{M}_\odot/pc^3$ for the local stellar mass density, which is a slight decrease compared to the $0.045\,\mathcal{M}_\odot/pc^3$ deduced from CNS2 (Wielen, 1974). This decrease is only partly due to the Hipparcos measurements. Also the maximum of the present LMF, which is only marginally influenced by Hipparcos, shows fewer stars than in 1983. Of course, recently detected free-floating brown dwarfs, e.g. Kelu-1, may increase the local stellar mass density significantly (Fuchs et al., 1998).

5 Kinematics

The impact of Hipparcos on the kinematics of the nearby stars is less conspicuous. In Jahreiß and Wielen (1983) two methods were applied to receive different age groups of nearby stars. In the upper part of the CM diagram, occupied by stars with masses larger than $1\,\mathcal{M}_\odot$, an age separation could be obtained by forming different B–V intervals. The mean age τ of such CM group is assumed to be about half the lifetime of a main-sequence star at the mean B–V of the group. The CNS4 allows to extend the completeness limit to 25 pc, which is a doubling of the volume or the number of stars with respect to the 20 pc used for CNS2. Yet, this doubling doesn't occur. Again the *cleaning* effect of Hipparcos removed about 20 per cent of the stars in the CNS2 groups 5 and 6. Nevertheless, this had only minor consequences for the resulting stellar kinematics.

In the lower part of the CM diagram also the CNS4 is no longer complete, and high-velocity stars are overrepresented. To avoid a kinematical bias the McCormick K and M dwarfs (Vyssotsky, 1963) were selected. For almost 300 of these stars O.C. Wilson estimated the CaII emission intensity at the H and K lines in a relative scale, and it turns out that increasing age implies decreasing HK intensity. Mean ages for the HK-groups were obtained from their relative frequencies under the assumption of a constant rate of star formation over the last 10^{10} years. A detailed definition of the CM and HK groups as well as results with respect to the dynamics of the Milky Way are given in Jahreiß et al. (1998).

The space velocity components U in the direction to the galactic center, V in the direction of galactic rotation, and W in the direction to the north galactic pole have been calculated with respect to the Sun. In Table 4 the resulting mean velocities and velocity dispersions are summarized. These have been obtained by weighting each star with its $|W|$-velocity, and are thus representative for a cylinder perpendicular to the galactic plane. The old giants and the early type stars (B–V ≤ 0.34) in the CM groups 6d, 6c, and 6b have $M_V \geq 4^m$. Therefore, the Hipparcos 'survey' provides the stars for an extension of the distance limit to 50 pc without any loss of completeness (for most of the additional stars also radial velocities were available). The

Table 4: *Mean velocities with respect to the Sun and velocity dispersions for CM groups and HK groups (|W|-weighted)*

n	group	$<U>$	$<V>$ [km/s]	$<W>$	σ_U	σ_V [km/s]	σ_W	σ_{tot}	τ [10^9 yr]
8	group 6d*	–8	–7	–10	15	7	3	17	0.21
15	group 6c	–7	–12	–15	16	15	4	22	0.47
19	group 6b	–10	–2	–1	16	11	9	21	1.0
78	group 6a	–3	–14	–17	30	22	16	40	2.3
149	group 5	–23	–29	–3	46	33	25	61	5.0
104	group 4	–15	–24	–5	44	30	19	56	5.0
174	group 3	–10	–21	–8	44	27	20	55	5.0
173	group 2	–10	–28	–4	42	27	23	55	5.0
361	group 1	–7	–27	–14	50	33	28	66	
600	group 5–2	–14	–26	–5	44	29	22	57	5.0
30	old giants	–9	–31	–10	29	31	21	48	7.0
15	subdwarfs	54	–191	31	112	83	66	154	10.0
12	white dwarfs	5	–21	6	41	25	13	49	
516	K + M dwarfs	–7	–26	–7	45	32	24	60	5.0
37	HK +8/+3	–10	–14	–1	22	11	7	25	.36
57	HK +2	–5	–17	–8	26	17	13	34	1.45
55	HK +1	0	–19	–7	35	21	17	44	3.17
57	HK 0	–5	–26	–6	46	21	17	54	5.19
34	HK –1	–5	–28	3	43	34	31	63	7.02
44	HK –2/–5	–2	–34	–11	65	35	28	79	8.91
60	group 6d (50 pc)	–10	–16	–6	16	10	5	20	0.21
95	group 6c (50 pc)	–12	–10	–7	19	12	7	23	0.47
168	group 6b (50 pc)	–12	–10	–5	23	13	8	27	1.0
215	old giants (50 pc)	–10	–33	–14	41	33	23	58	7.0

* two UMa cluster stars were combined

resulting enlarged groups are listed at the end of Table 4.

Figure 3 shows the total velocity dispersion as a function of the mean age of the groups. Here and in the following circles represent CM groups and triangles HK-groups. Open symbols represent CNS2 values, and filled symbols represent CNS4-values. The full line describes the increase of the velocity dispersion with age as expected from a diffusion process under the assumption of a constant diffusion coefficient (Wielen, 1977). It is obvious, that this theory is confirmed by the new values. Table 4 and Figure 3 show the odd behaviour of group 6b, whereas the enlarged group 6b fits much better.

Weighted means of the solar motion for all groups yield $U_\odot = +8.3 \pm 1.3$ km/s and $W_\odot = +8.0 \pm 1.4$ km/s. This is rather close to Delhaye's (1965) values $U^L_\odot = +9$ km/s and $W^L_\odot = +7$ km/s for the solar motion with respect to the LSR.

The asymmetric drift ΔV of a stellar population is defined as the difference between the circular velocity V_c and the mean rotation velocity V_Φ of this population. From the Jeans equations it can be deduced that the mean motion $\Delta V \propto \sigma^2_U$, and for $\sigma_U \rightarrow 0$ km/s it should approach the solar motion $V^L_\odot$ with respect to the LSR. This relation is plotted in Figure 4. Again group 6b but also the old giants show rather large deviations, that for the most part

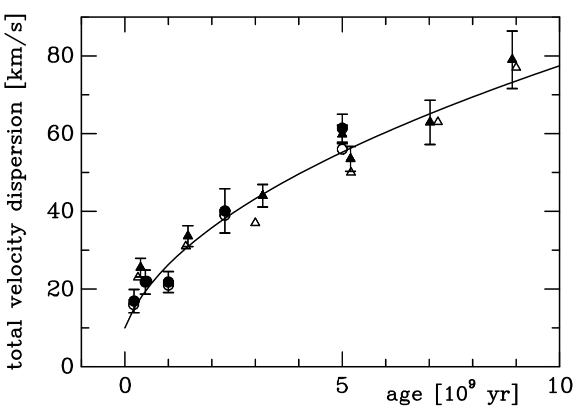

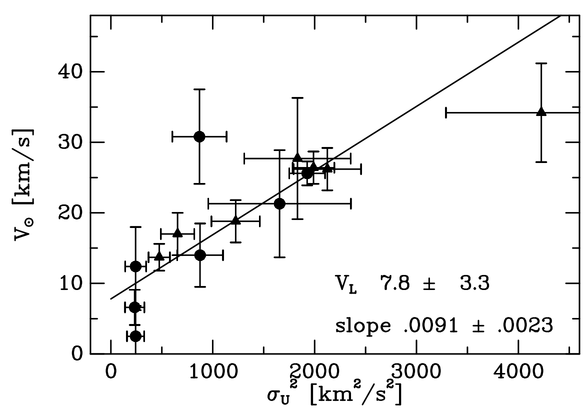

Figure 3: total velocity dispersion versus age. Figure 4: Asymmetric drift.
open symbols (CNS2), full (CNS4); circles (CM group), triangles (HK group)

could be removed in taking the enlarged 50 pc-samples. A more detailed analysis indicates that the old giants may be contaminated by clump giants, and these are probably much younger. Removing the old giants and the white dwarfs as well as the two youngest age groups, which are not yet in a dynamically relaxed state, a circular velocity of $V_\odot^L = 7.8 \pm 3.3$ km/s and a slope of 0.0091 ± 0.0023 are obtained (full line in Fig. 4). Then the radial exponential scale length becomes $h = 0.444 R_\odot = 3.8^{+1.1}_{-0.7}$ kpc or $h = 3.3^{+0.8}_{-0.6}$ kpc including a tilt term. These values are still at the upper end of other recent determinations (Sackett, 1997).

6 Conclusions

The astrometric satellite Hipparcos observed about 90 per cent of the *nearby* stars that were within the magnitude range accessible by the satellite, and added almost 200 new nearby objects and components. Consequently, the CNS4 which was compiled on the basis of the Hipparcos measurements achieved an unprecedented quality.

The bright part ($M_V \leq 8^m$) of the new nearby star sample is complete within a much larger volume than before. In addition, due to its very precise parallaxes Hipparcos *cleaned* up the bright portion of the colour-magnitude diagram, which represents now the true distribution of the massive stars within 25 pc and allows more precise studies of kinematics, metallicity and age effects.

Likewise, the bright end of the local stellar luminosity function could be determined with higher accuracy than before yielding a 15 per cent loss in star number density, and in a slightly lower stellar mass density of $0.039 \mathcal{M}_\odot pc^{-3}$.

Very probably we must wait for DIVA or GAIA to obtain a similar extraordinary improvement for the fainter stars not yet included in Hipparcos.

References

Delhaye, J. 1965, in: Galactic Structure, Stars and Stellar Systems 5, 61

ESA 1997, The Hipparcos and Tycho Catalogues, ESA SP-1200

Fuchs, B., Jahreiß, H., Flynn, C. 1998, A&A in press

Gliese, W. 1957, Astr. Rechen-Inst. Heidelberg, Mitt. A, No. 8 (CNS1)

Gliese, W. 1969, Veröff. Astr. Rechen-Inst. No. 22 (CNS2)

Jahreiß, H., Fuchs, B., Wielen, R. 1998, in *Dynamics of Galaxies and Galactic Nuclei*, Proc. Ser. ITA No.2, eds. Duschl, W. and Einsel, C., Heidelberg, in press

Jahreiß, H., Wielen, R., 1983, in IAU Coll. No. 76, L. Davis Press, Schenectady, 277

Jahreiß, H., Wielen, R., 1997, in *Hipparcos Venice'97.* ESA SP-402, 675

Sackett, P.D. 1997, ApJ 483, 103

van Altena, W.F., Lee, J.T., Hoffleit, E.D. 1995, The General Catalogue of Trigonometric Stellar Parallaxes, Fourth Edition, Yale University Observatory, New Haven

Vyssotsky, A.N. 1963, in: Basic Astronomical Data, Stars and Stellar Systems 3, 192

Wielen, R. 1974, IAU Highlights of Astronomy 3, 395

Wielen, R. 1977, A&A 60, 263

Wielen, R., Jahreiß, H., Krüger, R., 1983, in IAU Coll. No. 76, L. Davis Press, Schenectady, 163